IEEE Access
Multidisciplinary | Rapid Review | Open Access Journal

Received November 30, 2016, accepted January 8, 2017, date of publication February 14, 2017, date of current version May 17, 2017.

Digital Object Identifier 10.1109/ACCESS.2017.2669263

Study on Self-Tuning Tyre Friction Control for Developing Main-Servo Loop Integrated Chassis Control System

RONG-HUI ZHANG[1], ZHAO-CHENG HE[1], HAI-WEI WANG[2], FENG YOU[2], AND KE-NING LI[3]

[1]Guangdong Key Laboratory of Intelligent Transportation System, Research Center of Intelligent Transportation System, School of Engineering, Sun Yat-sen University, Guangzhou 510275, China
[2]School of Civil Engineering and Transportation, South China University of Technology, Guangzhou 510640, China
[3]State Key Laboratory of Mechanical System and Vibration, School of Mechanical Engineering, Shanghai Jiao Tong University, Shanghai 200240, China

Corresponding authors: H. Wang (whw2046@126.com) and K. Li (lkn_sjtu@126.com)

This work was supported in part by the Science and Technology Planning Project of Guangdong Province under Grant 2014B010118002, in part by the National Natural Science Foundation of China under Grant 51375298 and Grant 51208500, and in part by the National Key Technology R&D Program under Grant 2014BAG01B04.

ABSTRACT The inherent flexibility of hierarchical structure scheme with main-servo loop control structure is proposed to the problem of integrated chassis control system for the vehicle. It includes both main loop, which calculates and allocates the aim force using the optimal robust control algorithm and servo loop control systems, which track and achieve the target force using the onboard independent brake actuators. In fact, for the brake actuator, the aim friction is obtained by tracking the corresponding slip ratio of target force. For the coefficient of tire-road friction varying with different road surface, to get the nonlinear time-varying target slip ratio, the most famous quasi-static magic formula is proposed to estimate and predict real-time coefficient of different road surface and the constrained hybrid genetic algorithm (GA) is used to identify the key parameters of the magic formula on-line. Then, a self-tuning longitudinal slip ratio controller (LSC) based on the nonsingular and fast terminal sliding mode (NFTSM) control method is designed to improve the tracking accuracy and response speed of the actuators. At last, the proposed integrated chassis control strategies and the self-tuning control strategies are verified by computer simulations.

INDEX TERMS Main-servo loop control structure, parameters identification, tire-road friction control, constrained hybrid genetic algorithm, nonlinear sliding mode control.

I. INTRODUCTION

Today, a variety of active electronic control systems are used to improve the handling performance, comfort, active safety of the vehicle in complex driving conditions, such as antilock brake system (ABS) which is used to control the value of the braking force, so that the wheel is not locked in the edge of the maximum slip to ensure optimal braking force and stability of the of the vehicle [1]–[3], four wheel steering (4WS) which is designed to improve the handling performance and stability of the vehicle using the rear two wheel as the steering wheel, in addition to the traditional front wheel [4], [5] and electronic stability program (ESP) which using differential braking to improve vehicle stability based on ABS [6], [7], etc. However, most of the above electronic systems have focused on the single function optimization and can not solve the growing conflict between these systems, the integrated control which consolidates and optimizes more than two these systems has gradually become a research hotspot, and achieved a series of results, such combined system of active suspension system and ESP, active front steer angle control system and direct yaw moment control system [8]–[10]. Furthermore, significant developments in Intelligent Vehicles and Transportation Systems have been achieved during the last decade [11], [12], [53], which have improved the road safety, comfort, efficiency and intelligence [13]. By the vehicle-to-vehicle (V2V) communications using Dedicated Short Range Communications (DSRC), the vehicle gets information not only from itself, but the preview information of the front one which can drastically reduce oscillations and fuel consumption due to speed changes [14]–[16]. Based on the adaptive cruise control(ACC), cooperative adaptive cruise control (CACC) has been developing rapidly, which can effectively improve the traffic capacity, efficiency,

fluency [17]–[19]. For the extension of the Forward Collision Warning (FCW) only warning the potential collision risk with the obstacles or a moving vehicle in front of the vehicle toward the Advanced Emergency Braking System (AEBS) which can warn and control the vehicle when exists a potential collision risk using radar or camera information and effectively prevents accidents and reduces casualties simultaneously [20], [21]. Now, while one line of the vast majority of research projects centered on Advanced Driver Assistance Systems (ADAS) [11], the next step in the development of Intelligent Vehicles or Transportation Systems points toward the fully autonomous vehicles [22], [23].

Indeed, these studies really improve vehicle handling performance, active safety and comfort. However, most of them only afford to estimate of tire friction or total yaw moment, rather than their effective implementation [24], [25]. Little consideration is taken for the tyre-road friction generating principle and implementation [26]–[28]. While some of these studies have considered these factors and designed the control strategies, they are provided the only simple methods to allocate the yaw moment of the vehicle to brake forces in one single axle [29]–[31]. Consequently, the seemingly ideal control strategies and theoretical analysis results might probably be Utopia because of the ignorance of an overall consideration of the tyre–road saturation and interaction. For example, when a greater tyre force or body yaw torque is needed, simply increasing braking torque will make thing worse if the slip ratio of the tyre has been near or exceed the saturation area [7], [32]. So, the combined control logics are analyzed and designed to solve this problem [33]–[37]. However, with the rapid development of integrated control, since the realization of the tyre friction remains to be a key issue concerning the vehicle handling and stability performance and active safety.

In our previous studies, a hierarchical integrated control system with the main/servo loop is proposed to solve the problem of nonlinear interaction and coupling in vehicle dynamics control systems [38]–[41]. As an in-depth improvement and supplement, this paper focus on the control strategy to realize tyre friction identification and self tuning control in the servo loop [42], [43].

Furthermore, sliding-mode control (SMC) is a well-known efficient robust algorithm which has been widely applied for both linear and nonlinear systems [44]. This is an efficient robust algorithm for the dynamical systems with uncertainties. In general, an arbitrary linear manifold is considered as a sliding surface to guarantee the speed and accuracy performance of the closed-loop control system. However, the main disadvantage of SMC scheme is that the system states cannot reach the equilibrium point in finite time. But, in recent years, a new control scheme called terminal sliding-mode control (TSMC) is proposed to overcome this drawback utilizing nonlinear sliding surface [45], [46]. Nonlinear switching hyper planes in TSMC can improve the transient performance substantially. Besides, compared with the conventional SMC with linear sliding manifold, TSMC offers some superior properties such as faster, finite time convergence, and higher control precision. Furthermore, a non-singular fast terminal sliding mode (NFTSM) method is proposed to avoid the singularity in TSM control systems and have a good advantage in tracking time performance compared with other controllers, such as PID controller [47], [48], [63]–[65].

Then, Genetic Algorithm (GA) combined with sequential quadratic programming (SQP) algorithm is proposed to optimize the key parameter identification effect which combined with a variety of algorithm advantages, such as natural genetics, randomly structured information exchange and Darwinian 'survival of the fittest' theory [49], [50], Genetic algorithms (GA), first formulated by John Henry Holland (1975) [51], [52], offer an appropriate approach to optimization problems requiring efficient and effective global search processes. Specifically, the genetic algorithm consists of three key factors with different functions they are 'reproduction', 'crossover' and 'mutation'. The 'reproduction' obtained higher probabilities with breeding their copies in the new generation quickly. The 'crossover' selected portioning position of two chromosomes randomly to choose the better qualities among the preferred good strings and extend the genetic search space. The 'Mutation' reinforces the chance of reaching the optimal point using random heuristics. In the following, each binary numeric value of the strings of the actual parameters is decoded to be its decimal values and sent to objective function. Then, the optimal value of performance index is obtained and decoded to get the optimized parameters of the reference model [53]–[55].

Based on the above analysis, this paper is organized as follows: the proposed vehicle model is designed in section 2. The self-tuning friction controller is presented in section 3. The aim longitudinal slip ratio is calculated in section 4. The hierarchical integrated control system is presented in section 5. And, computer simulation and analysis results are shown in section 6.

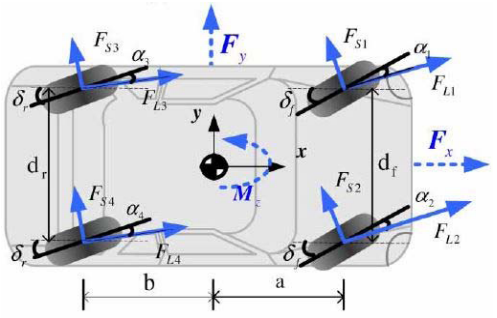

FIGURE 1. Vehicle model.

II. VEHICLE MODEL

In order to master the dynamic characteristics of the vehicle system, here, the vehicle dynamics mathematical model including longitudinal, lateral and yaw three degrees of freedom is established to design the integrated control system, as shown in Figure 1, without considering the aerodynamics,

ground slope and rolling resistance in the vehicle dynamics model in this interim work phase.

In the plane coordinate system, vehicle system dynamics equation be obtained as follows

$$\begin{bmatrix} m_v(\dot{u} - v\dot{\psi}) \\ m_v(\dot{v} + u\dot{\psi}) \\ I_z\dot{\psi} \end{bmatrix} = \begin{bmatrix} \sum\limits_{i=FL,FR,RL,RR} F_{x,i} \\ \sum\limits_{i=FL,FR,RL,RR} F_{y,i} \\ \sum\limits_{i=FL,FR,RL,RR} M_{z,i} \end{bmatrix} \tag{1}$$

where, $\sum F_{x,i}$ is the total vehicle longitudinal dynamics, $\sum F_{y,i}$ is the lateral force, and $\sum M_{z,i}$ is the yaw moment, which are essentially obtained by the interactions of the tyre–road and the inherent dynamics of the vehicle implicitly expressed by the combined slip magic tyre model which, as a best fit between experimental data and theoretical model, can produce typically lateral and longitudinal force and self-aligning torque of the vehicle at the contact patch [28].

III. CONTROL STRUCTURE OF SELF-TUNING TYRE-ROAD FRICTION FORCE CONTROLLER

In the hierarchical integrated control system, whose structure is diagrammatized in Figure 3, self-tuning tyre-road friction force controller and active steering control system is designed to track the aim control force and aim steering angle as the servo actuators. In this section, self-tuning braking force controller is used to calculate and track the allocated tyre friction from the upper layer controller. Here, we mainly focus on the longitudinal tyre friction control.

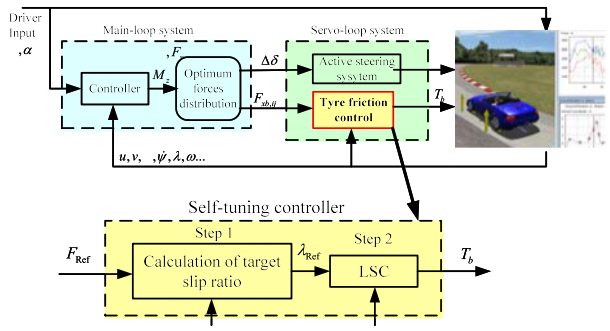

FIGURE 2. Schematic diagram of hierarchical integrated control system and self-tuning controller.

For the existing nonlinear time, varying characteristics between the slip ratio and the tyre-road friction force during the different road surface, it is difficult to directly obtain the corresponding slip ratio of the desired friction force. So, as showed in Figure 2, two steps are included in the self-tuning controller. First of all, the reference tyre-road friction model is established based on the magic formula to predict the slip rate changing with the tire force. Its key varying parameters is identified on-line using constrained hybrid genetic algorithm (GA). Then, the aim ratio slip of the desired friction is calculated via the numerical method. This means the controller is endowed to the ability of self-tuning to road variations through this process. Next, LSC is provided to track the calculated slip ratio rapidly and precisely based the exerting brake system using the nonsingular and fast terminal sliding mode (NFTSM) algorithm.

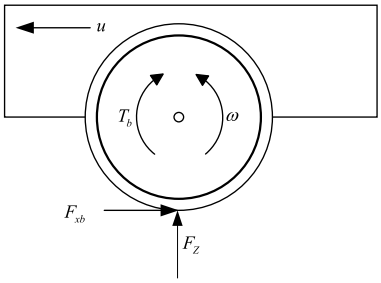

FIGURE 3. Schematic of quarter-car model.

IV. ESTIMATION OF DESIRED SLIP RATIO

A. QUARTER-CAR MODEL

The LuGre model is popular because its parameters have a physical significance and its velocity-dependency is also physically consistent. However, the quasi-static value of the aim slip is necessary for the controller design of ABS. So, the alleged Magic formula is the root of the reference tire model in this paper. In terms of research on vehicle dynamics, it is an extensively used semi-empirical tire model which be used to calculate steady-state tire force and moment characteristics. In order to master the dynamic characteristics of braking system and estimate the tyre-road friction, a quarter-car model is established, as shown in Figure 3. For the previous studies, there has been an attempt to measure the brake torque of conventional vehicles by force transducer mounted on the brake caliper support [3], [58], [59], here, the brake torque is measured by transducers mounted in Electronic Brake System(EBS) is designed to control brakes through electrical means using brake-by-wire technology. Then, the tyre friction can be calculated using the following method.

The dynamic equations of the quarter-car model are shown as follows:

$$m\frac{du}{dt} = -F_{xb} \tag{2}$$

$$J\frac{d\omega}{dt} = r_b F_{xb} - T_b \tag{3}$$

$$F_Z = mg \tag{4}$$

Where,

m	is the mass of the quarter-car
u	is the vehicle speed
F_{xb}	is the tyre-road friction
J	is the wheel inertia
ω	is wheel angular speed
r_b	is wheel radius
T_b	is brake torque
F_Z	is vertical force of the vehicle
g	is acceleration of gravity

The tyre-road friction force can be calculated by the following equation:

$$\hat{F}_{xb} = \frac{J}{r_b}\frac{d\omega}{dt} + \frac{T_b}{r_b} \tag{5}$$

And the longitudinal desired slip ratio $\hat{\lambda}_{xb}$ with respect to $\hat{F}_{xb}$ is estimated by

$$\hat{\lambda}_{xb} = \frac{u - \omega r_b}{u} \tag{6}$$

The equation (7) is deduced to describe the non-linear relationship of the tyre-road friction F_{xb} and the corresponding ratio slip λ_{xb}

$$F_{xb} = F_Z \cdot \mu_{xb}(\lambda_{xb}) \tag{7}$$

where μ_{xb} is tyre-road coefficient.

V. REFERENCE TYRE MODEL

In this paper, the most famous magic formula is proposed as the reference tyre model to study the basic principles of tire-road force [28]. It is a widely used semi-empirical tyre model to calculate steady-state tyre force and moment for the vehicle dynamics studies. The general form of the formula that holds for given values of vertical load and the longitudinal dynamics can be get as the following

$$\begin{aligned}\mu_L &= \mu(\lambda, B_L, C_L, D_L, E_L) \\ &= D_L \sin[bC_L \arctan\{B_L\lambda - E_L(B_L\lambda - \arctan(B_L\lambda))\}]\end{aligned} \tag{8}$$

where

μ_L	the tyre-road friction coefficient
λ	the ratio slip
B_L	stiffness factor of the magic formula
C_L	shape factor of the magic formula
D_L	peak value of the magic formula
E_L	curvature factor of the magic formula

Usually, the driving conditions of vehicle are changeable, e.g., the variation of road surface. So, the varying parameters of Magic formula B_L, C_L, D_L and E_L should be estimated on-line.

A. CONSTRAINED HYBRID GENETIC ALGORITHM FOR REFERENCE TIRE MODEL PARAMETERS IDENTIFICATION

The weighted sum of squares of the error of the estimated value and the true value $\hat{F}_{xb,i}$ of the tire-road friction force is presented as the optimization index to minimize the error of the estimated value and the true value of B_L, C_L, D_L and E_L, as shown in the equation(9). Then the above parameter identification problem is converted to a constrained optimization problem, we get

$$\min_x PI = \sum_{i=1}^{N} w_i \left[\hat{F}_{xb,i} - F_Z\mu\left(\hat{\lambda}_{xb,i}, x^T\right)\right]^2$$

$$x = [B_L, C_L, D_L, E_L]^T \tag{9a}$$

$$s.t.\ x_{\min} \le x \le x_{\max} \tag{9b}$$

where w_i weighting factor of optimization index $x_{\min}$ and $x_{\max}$ are respectively the maximum and minimum constrained range for B_L, C_L, D_L and E_L.

In this section, constrained hybrid genetic algorithm, which takes the advantage of each other of Genetic Algorithm (GA) and the active-set sequential quadratic programming (SQP) method, is proposed to minimized the PI. The advantage of GA is that it can reach the region near an optimum point relatively quickly. However, the lack of algorithm is it can take many function evaluations to achieve convergence [47], [48]. On the contrary, SQP can achieve convergence near an optimum point quickly. So, the hybrid algorithm is designed to run GA for a small number of generations to get near an optimum point. Then the solution from GA is used as an initial point for SQP approach which is faster and more efficient for local search [55], [56].

As described above, the GA is proposed to calculate and search the optimal values of B_L, C_L, D_L and E_L. Their encoded binary string of fixed length can be get as the following

$$\underbrace{\overbrace{B_L}^{S_1}, \overbrace{C_L}^{S_2}, \overbrace{D_L}^{S_3}, \overbrace{E_L}^{S_4}}_{string}$$

Each value of B_L, C_L, D_L and E_L are encoded as N1,N2, N3 and N4 bits respectively. Then, we get the whole length of the string, i.e., the chromosome in GA for the optimization calculation process, have a total of N1+N2+N3+N4 bits. It gets that, if

$$\begin{aligned} S_1 &= \underbrace{10\cdots0100100}_{N1bits} \\ S_2 &= \underbrace{00\cdots010101}_{N2bits} \\ \cdots &\quad \cdots \\ S_4 &= \underbrace{10\cdots000101}_{N4bits} \end{aligned}$$

then the decoded decimal values of B_L, C_L, D_L and E_L are given as

$$\begin{aligned} B_L &= B_{L,\min} + \frac{d_{B_L i}}{2^{N1}-1}\left(B_{L,\max} - B_{L,\min}\right) \\ C_L &= C_{L,\min} + \frac{d_{C_L i}}{2^{N2}-1}\left(C_{L,\max} - C_{L,\min}\right) \\ \cdots &\quad \cdots \\ E_L &= E_{L,\min} + \frac{d_{E_L i}}{2^{N4}-1}\left(E_{L,\max} - E_{L,\min}\right) \end{aligned}$$

where, $d_{B_x i}$, $d_{C_x i}$, …, $d_{E_x i}$ respectively represent the binary value for B_L,C_L,…,E_L [53], [57].

Furthermore, several key genetic parameters during GA-based searching procedure, such as generation number, population size, the crossover rate et al. is described in section 6, in addition to encoding the parameters and derivation of performance index(PI).

Active set SQP subject to the near-optimal region nonlinear inequalities constrained optimization algorithm is provided

as the combined function with GA for the hybrid genetic algorithm [59], [60].

In order to establish the mathematical formula of the optimization algorithm, the upper and lower bound constraints mathematical formula, as shown in equation (9a), can be transformed into common inequality constraints as following

$$A_c x \geq b_c \tag{10}$$

$$A_c = [I, -I]^T, b_c = [x_{\min}, -x_{\max}]^T \tag{11}$$

Where, $I \in R$ is 4×4 identity matrix.

Then the Lagrangian equation of the upper and lower bound constrained problem (9) can be get as

$$L(x, \varphi) = PI(x) - \sum_{i \in \psi} \varphi_i (\alpha_i x - b_i) \tag{12}$$

where $i \in \psi$ are the inequality constraints as described in the equation (10). The active set for any feasible x is defined as

$$A_a(x) = \{i \in \psi | A_c x \geq b_c\} \tag{13}$$

For Lagrangian equation cannot be used to solve the inequality-constraints optimization problem (9) , the active set SQP algorithm is extended for the equality-constrained problem transformed from the inequality-constrained one. Firstly, the so-called working set $I^{(k)}$ is selected from a subset of constraints at each iteration $x^{(k)}$ by the proposed algorithm. Then, the proposed algorithm solves only equality-constrained subproblems, the constraints in the working sets are imposed as equalities and all other constraints are ignored. The proposed algorithm updates the working set of the constraints at every iteration by designed rules.

Suppose the updated set at the iterate $\left(x^{(k)}, \varphi^{(k)}\right)$, we can get the quadratic programming as following

$$\min q(p) = \nabla PI_k^T p + \frac{1}{2} p^T W_k p \tag{14a}$$

$$s.t.\ A_k^T p + A_c(x_k) - b_c \geq 0 \tag{14b}$$

At the working set $I^{(k)}$, the equality-constraints optimization problem is solved as the following equation:

$$\min\ \nabla PI_k^T p + \frac{1}{2} p^T W_k p$$

$$s.t.\ a^i p + A_c^i \left(x^{(k)}\right) - b_c^i = 0, i \in I^{(k)} \tag{15}$$

Define

$$\delta = p - p^{(k)} \tag{16}$$

We get

$$q\left(\delta + p^{(k)}\right) = \nabla PI_k^T \delta + \frac{1}{2} \delta^T W_k \delta + q\left(p^{(k)}\right) \tag{17}$$

where $q\left(p^{(k)}\right)$ is independent of q.

For, without changing the solution of the above optimization problem, the value $q\left(p^{(k)}\right)$ can be dropped from the objective, the QP subproblem can be solved at the *kth* iteration as:

$$\min\ \nabla PI_k^T \delta + \frac{1}{2} \delta^T W_k \delta \tag{18a}$$

$$s.t.\ a^i \delta = 0, i \in I^{(k)} \tag{18b}$$

If, at the iteration that the optimal δ_k from (18a) is nonzero, the step value of move along this direction need to be decided for the next step. If $p_k + \delta_k$ is feasible to all the constraints, set $p_{k+1} = p_k + \delta_k$. Otherwise, we set

$$p_{k+1} = p_k + \alpha_k \delta_k \tag{19}$$

To maximize the decrease in q, we want α_k to be as large as possible in the range of [0, 1] subject to retaining feasibility, we get

$$\alpha_k \overset{def}{=} \min\left(1, \min_{i \notin I^{(k)}, a^i \delta < 0} \frac{b_{c,i} - a_{c,i}^T p_k}{a_{c,i}^T \delta_k}\right) \tag{20}$$

The value of W_k as an approximation of the Hessian of the Lagrangian is a key parameter and a choice for Any SQP calculation method in the quadratic model. A quasi-Newton approximation can be used as a way to approximate the Hessian of the Lagrangian, such as the BFGS, which updates the formula with Hessian approximation B_k rather than W_k, we have

$$s_k = x_{k+1} - x_k$$

$$y_k = \nabla_x L(x_{k+1}, x_{k+1}) - \nabla_x L(x_k, x_k) \tag{21}$$

$$B_{k+1} = B_k - \frac{B_k s_k s_k^T B_k}{s_k^T B_k s_k} + \frac{y_k y_k^T}{s_k^T y_k} \tag{22}$$

Using this approximation method, if $\nabla_{xx}^2 L$ is positive at the sequence of points x_k, the above method will converge rapidly; However, if $\nabla_{xx}^2 L$ is not positive, this approximation method may not work well.

So, an improved approximate method named damped BFGS updating for SQP was devised to ensure that the update is always well-defined. Using this idea, we have

$$r_k = \theta_k y_k - (1 - \theta_k) B_k s_k \tag{23}$$

where the scalar θ_k is defined as

$$\theta_k = \begin{cases} 1, & if\ s_k^T y_k \geq 0.2 s_k^T B_k s_k \\ \dfrac{0.8 s_k^T B_k s_k}{s_k^T B_k s_k - s_k^T y_k}, & if\ s_k^T y_k < 0.2 s_k^T B_k s_k \end{cases} \tag{24}$$

Update B_k as the following equation

$$B_{k+1} = B_k - \frac{B_k s_k s_k^T B_k}{s_k^T B_k s_k} + \frac{r_k r_k^T}{s_k^T r_k} \tag{25}$$

This method ensures that the updated B_{k+1} is positive definite [61], [62].

As above analysis, the chart of the constrained hybrid GA is shown as Figure 4.

VI. MAIN-SERVO LOOP INTEGRATED CONTROL DESIGN

In this section, upper control system of the hierarchical integrated control system is implemented into the main-servo-loop hierarchical control problems, including the design of main-loop controller, the forces and moment optimal distribution system and LSC controller which is shown in Figure 3.

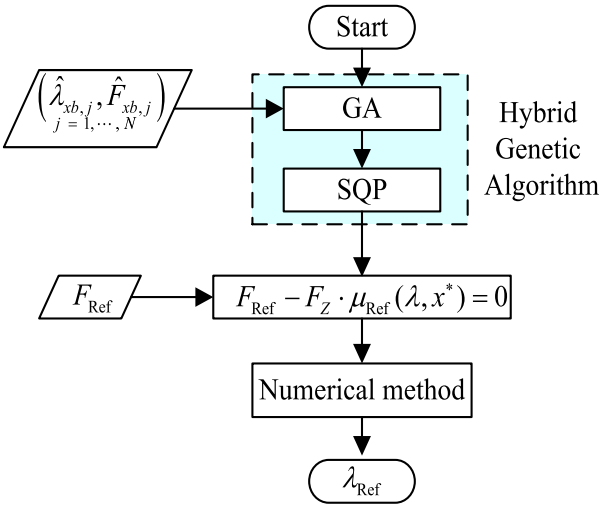

FIGURE 4. Flow chart of the estimation of desired slip ratio.

A. MAIN-LOOP CONTROL SYSTEM

According to the inherent dynamic characteristics of automotive, in order to ensure the vehicle stability, its side-slip angle should be made as small as possible. Meanwhile, the absolute value of the error between the desired yaw rate and its real value should be as small as possible. It is achieved by the main-loop controller which is designed to track the reference model $[v = 0, \dot{\psi} = \dot{\psi}_d]^T$ of the vehicle with three degrees of freedom.

The desired yaw rate $\dot{\psi}_d$ can be obtained using the designed understeer characteristics and nominal longitudinal velocity u_0 as

$$\dot{\psi}_d = \frac{1}{1 + K(u_0^2/Lg)} \frac{u_0}{L} \delta_D \tag{26}$$

with the constraint

$$\left|\dot{\psi}_d\right| \leq \left|\frac{u_{Ref}}{u_0}\right| g \tag{27}$$

where K is nominal understeer characteristic value and L is wheelbase of the vehicle.

Here, using the vehicle characteristics at the external inputs, the vehicle dynamics equations (1) can be linearized into the state-space form as

$$\dot{X} = AX + B_1 w_1 + B_2 w_2 \tag{28}$$

where, the motion state deduced from steady state values are defined as the state vector X

$$X = \left[\Delta u, \Delta v, \Delta\dot{\psi}\right]^T$$

with the external disturbances introduced from the same channels as $w_1 = \left[\bar{F}_x^w, \bar{F}_y^w, \bar{M}_z^w\right]^T$.

The errors of interest between the real values and the desired ones can be suppressed using the feedback controller. With a similar principle, a standard H_∞ regulation system is designed to a weighted system model based on equation (28) and

$$\begin{bmatrix} \begin{bmatrix} z_1 \\ z_2 \end{bmatrix} \\ y \end{bmatrix} = \begin{bmatrix} \begin{bmatrix} W_{pp}p_0 W_{wu} & 0_{2\times 2} \\ 0_{3\times 3} & 0_{3\times 2} \end{bmatrix} \begin{bmatrix} W_{pp}p_0 \\ W_{pu} \end{bmatrix} \\ \begin{bmatrix} p_0 W_{wu} & W_n \end{bmatrix} \quad p_0 \end{bmatrix} \times \begin{bmatrix} \begin{bmatrix} w_1 \\ w_2 \end{bmatrix} \\ u \end{bmatrix} \tag{29}$$

with respect to the performance vector

$$\bar{z}_1 = \left[\Delta u, \Delta v, \Delta\dot{\psi}\right]^T$$

In equation (29), p_0 is the nominal plant value which is determined by equation (28). The measurement values are assumed to be the same as $\bar{z}_1$ which is obtained from sensors and estimation. z_1 and z_2 are the weighted performance vectors z_2. W_{pp} and W_{pu} are defined as the weighting matrices for the motion performance and control magnitude constraints respectively; W_{wu} and W_n are provided as the weighting matrices for input value disturbances and measurement noise respectively.

Due to the resultant H_∞ norm of the above closed-loop system, the corresponding value K the H_∞ controller can be calculated for the total forces and yaw moments which is used for vehicle motion control. It is shown as follow

$$F_{ud} = u_c = \left[\bar{F}_x^{H\infty} \bar{F}_y^{H\infty} \bar{M}_z^{H\infty}\right]^T \tag{30}$$

B. FORCES AND MOMENTS OPTIMAL DISTRIBUTION SYSTEM

Coupling interaction between the vehicle and the different road surface, the allocation of the F_{ud} to the four independent actuator can be described as a nonlinearly constrained optimization problem, which is constrained by the tyre–road adhesion constraints, rate/magnitude limits and so on. Using the sequential quadratic programming (SQP) approach, the original constrained optimization problem is transformed in to an unconstrained programming problem, in which the changing rates and the magnitudes of actuator inputs are suppressed to the minimum level.

Then, the weighted cost function J_{SQP} is established as

$$J_{SQP} = E^T W_E E + \Delta u_c^T W_{\Delta u} \Delta u_c + u_c^T W_{\Delta u} u_c \tag{31}$$

where the force tracking errors $E = F_{ud} - F_u$ are the difference between desired value and actual value of vehicle control forces; Δu_c are the tyre variable magnitudes, which are described as the equation

$$\Delta u_c = [\Delta F_{x,FL}, \Delta F_{x,FR}, \Delta F_{x,RL}, \Delta F_{x,RR}, \Delta\alpha_{x,F}, \Delta\alpha_{x,R}]^T \tag{32}$$

while W_E, $W_{\Delta u}$ and W_u are weighting matrices.

At the$(K+1)$ $(K+1)$th time step, get the equations:

$$u_c(K+1) = u_c(K) + \Delta u_c \tag{33}$$

$$F_u(K+1) \approx F_u(K) + J_{cob}\Delta u_c \tag{34}$$

Where, the corresponding Jacobian matrix J_{cob} is obtained as the following

$$J_{cob} = \frac{\partial F_u}{\partial u_c} \tag{35}$$

For $J_{SQP}$is the cost function and should be minimized with respect to the control input variable u_c, it can be deduced as

$$\frac{\partial J_{SQP}}{\partial u_c} = 0$$

With the Equations (33) and (34), the allocated tyre variables can be solved from the following equation

$$\Delta u_c^d = \left(W_u + W_{\Delta u} + J_{cob}^T W_E J_{cob}\right)^{-1} \times \left[J_{cob}^T W_E \tilde{E} - W_u u_c\,(k)\right] \tag{36}$$

where $\tilde{E} = \bar{F}_u - F_u(k)$ is the error of the stabilizing forces between the desired and the current values.

Finally, through LSC which is mainly focused on in this paper and active steering system, the obtained optimal tyre variables from Equation (36) will be further converted into tyre control inputs, i.e. wheel torques and active steering angles and will be implemented using these active actuators.

C. LSC USING NFTSM

In this section, self-tuning controller for the slip ratios is presented using the non-singular fast terminal sliding mode (NFTSM) control algorithm, which has great robustness to measurement parameter uncertainties and input variables disturbances [63]–[65]. The control tracking accuracy and response speed can be improved greatly for the reason that the NFTSM maintains linear convergence when the value of sliding mode surface far away from the equilibrium and speeds up to converge with a non-linear characteristic when the value in the range of near the stable convergence point. Furthermore, it can avoid the singularity in control systems compared with fast terminal sliding mode (FTSM) and can converge in finite time compared with general sliding mode control.

The design details are described in the following paragraphs.Firstly, the time-varying sliding mode surface is defined as:

$$s = \dot{e} + \alpha e + \beta e^{\frac{p}{q}} \tag{37}$$

where $e \in R; \alpha, \beta$ are constant and $\alpha > 0; p, q$ are the positive odd integers and $p < q < 2p$.

The error of the longitudinal slip rate is defined as:

$$e = \lambda - \lambda_{\text{Ref}} \tag{38}$$

Combining the equation (5), (6) and (38), we get

$$\dot{e} = \frac{\frac{-r_b^2 F_{xb}}{J} + (1-\lambda)\,\dot{u}}{u} + \frac{T_b r_b}{uJ} - \dot{\lambda}_{\text{Ref}} \tag{39}$$

For the sliding mode control algorithm, which usually employ the discontinuous switch control method to deliver a finite time reachability of the controller, there are two phases named the reaching phase and the sliding phase must be taken during the control process. However, it is one of the major contributors to the ''chattering'' behaviors well known existed in sliding mode control. In this section, a well-designed 'nonlinear terminal attractor' is applied to develop a chattering free NFTSM controller, which is shown as follows

$$\dot{s} = (-\phi s - \gamma s^{\frac{m}{n}}) e^{\frac{p}{q}-1} \tag{40}$$

where $\phi \in R^+; \gamma \in R^+$, are tunable parameters to adjust the corresponding variable weights; m and n are the given positive odd integers and $0 < m/n < 1$. Combined the equations (37), (38),(39) and (40), the NFTSM control law can be obtained as:

$$T_b = \frac{u \cdot J}{r_b}\left\{\frac{q}{\beta \cdot p}\left(-\ddot{e} \cdot e^{1-\frac{p}{q}} - \alpha \cdot \dot{e} \cdot e^{1-\frac{p}{q}} - (-\phi s - \gamma s^{\frac{m}{n}})\right) - \frac{\frac{-r_b^2 F_{xb}}{J} + (1-\lambda)\,\dot{u}}{u} - \dot{\lambda}_{\text{Ref}}\right\} \tag{41}$$

Where

$$\ddot{e} = \frac{1}{u}\left\{-\ddot{\omega} \cdot r_b^2 - \frac{\frac{-r_b^2 F_{xb}}{J} + (1-\lambda)\,\dot{u}}{u}\,\dot{u} + \frac{T_b \cdot r_b}{u \cdot J}\dot{u} + (1-\lambda)\,\ddot{u}\right\} - \frac{(1-\lambda)\,\dot{u}^2}{u^2} - \ddot{\lambda}_{\text{Ref}} \tag{42}$$

For $0 < 1 - \frac{p}{q}$, from the equation (40), the proposed control system is able to converge to equilibrium following the sliding surface, without the singularity problem. And, from the equation(41), we get that the NFTSM control law can be effectively reduced the ''chattering'' phenomenon for the proposed control law is a time continuous variable without the discontinuous function term similar to $k \cdot sign(x)$ which is used in SMC.

Where $k \cdot sign(x) = \begin{cases} k, x > 0 \\ 0, x = 0 \\ -k, x < 0 \end{cases}$ and k is a constant.

From equation(42), high frequency variables, such as $\ddot{\omega}$ and $\ddot{u}$, are estimated from the measurement ω and estimated term u , the noise should be considered in those terms for application. For the paper focus is on paying more attention to the overall theoretical design of the proposed self-tuning integrated controller, the effect of noise measurements can be temporarily ignored which will be implemented in the next work.

From equation $s = 0$, it can be deduced as:

$$e^{-\frac{p}{q}}\dot{e} + \alpha e^{1-\frac{p}{q}} = -\beta \tag{43}$$

Let $z = e^{1-\frac{p}{q}}$, have:

$$\frac{dz}{dt} + \frac{q-p}{q}\alpha z = -\frac{q-p}{q}\beta \tag{44}$$

when $e = 0$,$z = 0$,$t = t_{si}$.

Solving the equation (44), t_{sar} can be deduced as the following:

$$t_{si} = -\frac{q}{\alpha\,(q-p)} \ln \frac{\alpha x(0)^{\frac{q-p}{q}} + \beta}{\beta} \tag{45}$$

Obviously, from the equation (45), t_{si} is a finite value. The analytical result indicates that the designed controller can reach the system equilibrium and converge in finite time.

VII. SIMULATIONS RESULTS AND ANALYSIS

In order to verify the validity of the proposed systems, we conducted a simulation lab using the tool of Carsim, Matlab/Simulink and the simulation in this part. The controller of LSC is designed using the Matlab/Simulink and the vehicle model is proposed using the Carsim, which is used worldwide by over 110 OEMs and Tier 1 suppliers and over 200 universities and government research labs. Firstly, the tracking performance of LSC is simulated and analyzed and the superiority and differences of the NFTSM is compared with NTSM. Then, the overall system performance of the self-tuning friction control is verified under different μ-jump road surface.

TABLE 1. Parameters of different road surface.

Road	B_L	C_L	D_L	E_L
Snow	17.430	1.4500	0.20	0.6500
Cobblestone,wet	14.027	1.4500	0.40	0.6000
Asphalt,wet	15.635	1.6000	0.80	0.4500
Cobblestone,dry	10.695	1.4000	0.85	0.6450
Concrete,dry	13.427	1.6402	0.97	0.5372
Asphalt,dry	13.427	1.5500	1.10	0.5327

The key parameters of the Magic Formula for several different typical road surfaces are provided in Table 1 and are shown in figure 5. Due to these parameters information of the different road surface, the constrained range of B_L, C_L, D_L and E_L, can be obtained respectively. The overall key parameters of the vehicle used in the following simulations are provided in Table 2.

A. VERIFICATION OF PARAMETERS IDENTIFICATION

Given the sampling points$\hat{F}_{xb}$ and $\hat{\lambda}_{xb}$, the simulation is carried out to verify the effectiveness and efficiency of the proposed identification scheme. The real parameters of tyre model are $B_L = 13.427$,$C_L = 1.6402$, $D_L = 0.97$ and $E_L = 0.5372$, and the identified values are $\hat{B}_L = 15.9205$, $\hat{C}_L = 1.4655$, $\hat{D}_L = 0.9701$ and $\hat{E}_L = 0.3438$. Then, the relationships between slip ratio and adhesion coefficient using above two sets of parameters are shown in Figure 6. It can be concluded that the accuracy of identification process can be ensured by the proposed hybrid GA method.

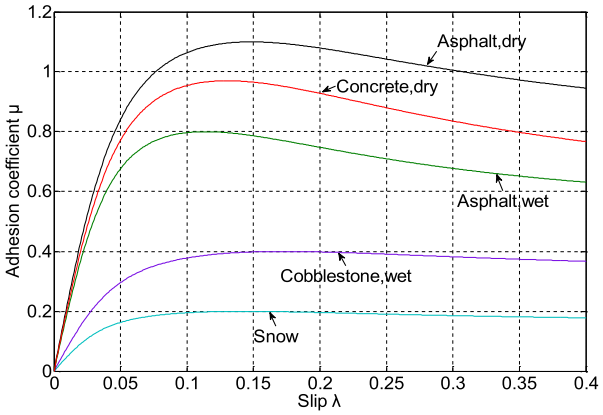

FIGURE 5. $\mu - \lambda$ curve of different road surface.

TABLE 2. Parameters used in simulations.

Notation	Value	Unit
m mass of quarter-car	382.5	kg
u vehicle velocity	120	km/h
g acceleration of gravity	9.8	m/s^2
J wheel inertia	12	$kg \cdot m^2$
r_b wheel radius	0.25	m
N_{data} number of sampling points	10	-
$B_{L,\min}$ lower bond of stiffness factor	8	-
$C_{L,\min}$ lower bond of shape factor	1	-
$D_{L,\min}$ lower bond of peak value	0.1	-
$E_{L,\min}$ lower bond of curvature factor	0.1	-
$B_{L,\max}$ upper bond of stiffness factor	18	-
$C_{L,\max}$ upper bond of shape factor	1.7	-
$D_{L,\max}$ upper bond of peak value	1.5	-
$E_{L,\max}$ upper bond of curvature factor	0.9	-
GA: initial population size	30	-
GA: max number of generation	100	-
GA: crossover rate	0.2	-
GA: mutation rate	0.8	-

B. VERIFICATION OF LSC TRACKING PERFORMANCE

The desired value of $\lambda_{\text{Ref}} = 0.19$ is given to the LSC controller to testify the tracking performance of the non-singular fast terminal sliding mode control system, the result is shown in Figure 7. It can be concluded that the NFTSM has shorter response time and higher control accuracy than NTSM. Furthermore, the proposed nonlinear control system is continuous and avoid the singular phenomenon effectively.

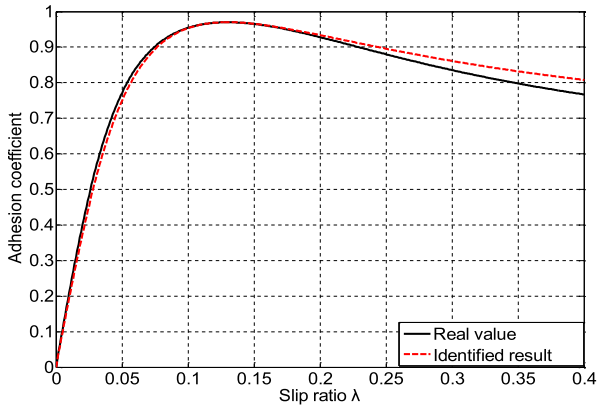

FIGURE 6. Relationships between slip ratio and adhesion coefficient.

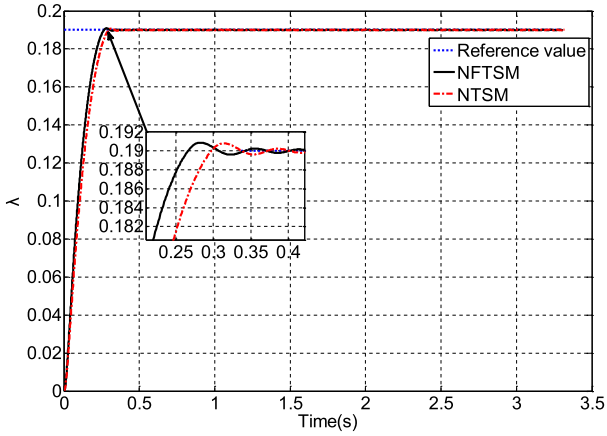

FIGURE 7. LSC tracking ability.

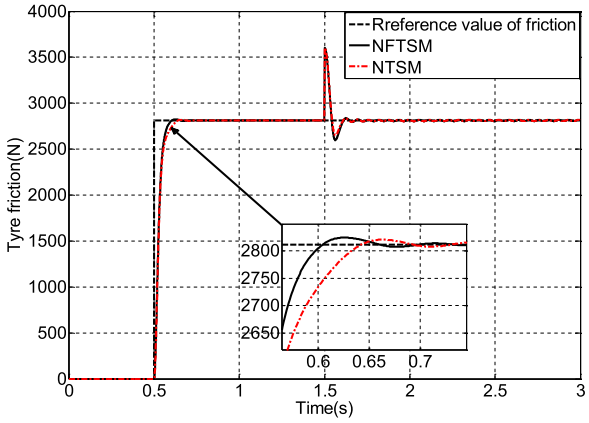

FIGURE 8. Tracking performance of tyre friction.

C. SIMULATION UNDER μ-JUMP ROAD CONDITIONS

In this section, the simulation is designed for the vehicle under μ-jump road conditions. The step reference tyre friction F_{Ref} input value is 2624N after 0.5s. And at 1.5s, the vehicle drives from asphalt, dry road to asphalt, wet road. The results of the simulation are shown in Figures 8∼10.

As shown in Figure 8 and Figure 9, the response of the nonsingular fast terminal sliding mode controller,

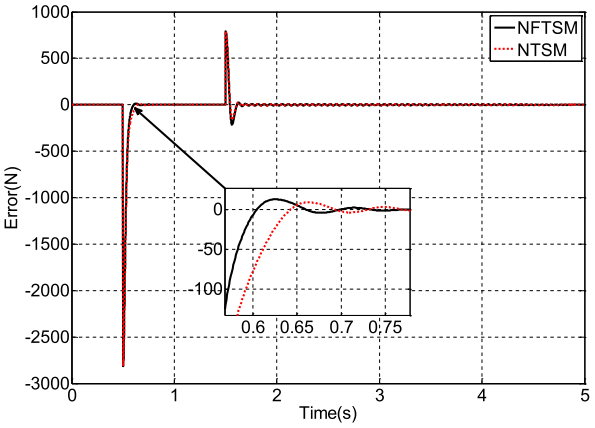

FIGURE 9. Tracking error of tyre friction.

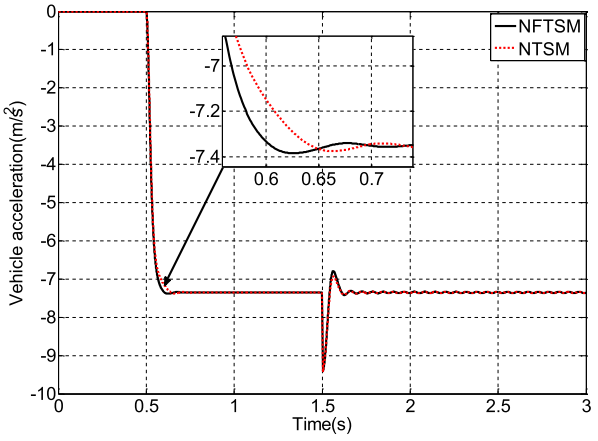

FIGURE 10. Vehicle acceleration.

which combines the advantage of the tracking factor of the linear term $\dot{e} + \alpha e$ and the nonlinear fractional term $\beta e^{p/q}$ to obtain an optimal control variable after 0.5s and 1.5s. Similarly, the response performance of vehicle acceleration of NFTSM is also more sensitive than that of NTSM, which is shown in Figure 10. The simulation results show the designed control system to be effective in tracking desired tyre friction and in adaptation to the variation in road surface.

D. SIMULATION RESULTS OF MAIN-SERVO LOOP SYSTEM WITH THE SELF-TUNING LSC UNDER STEP STEER MANOEUVRE

In this section, the vehicles with the proposed controller with a 120 km/h forward speed on a dry road, are subjected to a step steer input angle at 0.3 sec, with a front wheel steering angle of6°. For comparison, the simulation is carried out for three different configurations respectively, i.e. for the vehicle equipped with self-tuning LSC only, for the vehicle with 4WS only, and for the vehicle with INT equipped with a combination of the above two subsystems. The vehicle dynamic responses results are shown in Figures 11 ∼ 15.

Figure 11-12 show the simulation resultants of yaw rate and side-slip responses of the vehicle with different controller

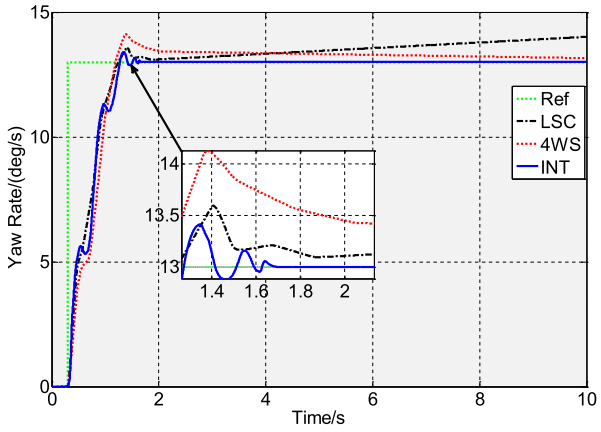

FIGURE 11. Yaw rate.

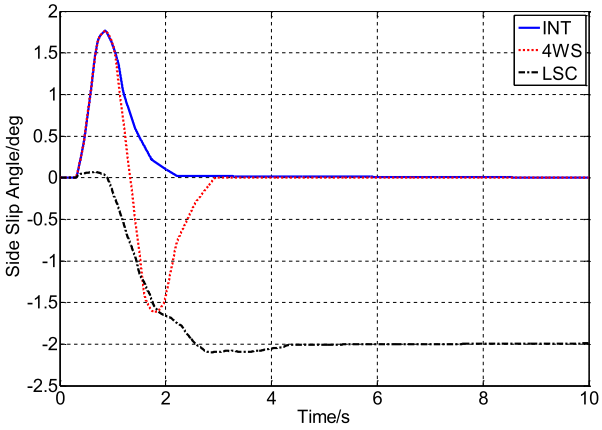

FIGURE 12. Side slip angle.

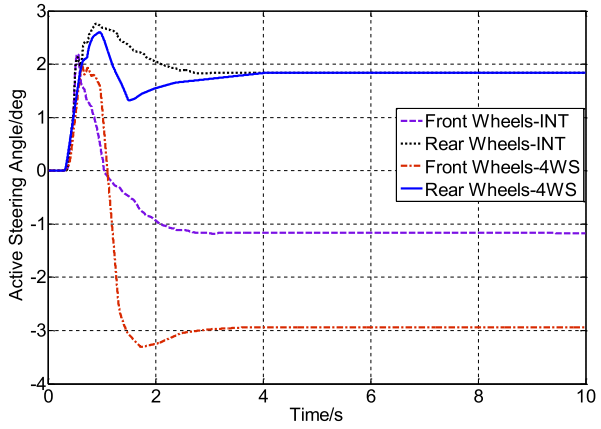

FIGURE 13. Active steering angle.

respectively, the simulation results show that, for the self-tuning LSC configuration, the steady state tracking errors are evident and, for the 4WS configuration, a large response overshoot is demonstrated while, for the INT configuration, both the nominal yaw rate tracking and the side-slip angle suppression performances are significant.

Since the vehicle motion upper layer designs are the same for three configurations, the greatly improvement in vehicle performance for control integration is obvious from the sub-system control coordination based on force and moment optimal distribution among the four wheels. Furthermore, this also shows the designed self-tuning tyre friction control system to be effective in tracking desired tyre-road friction.

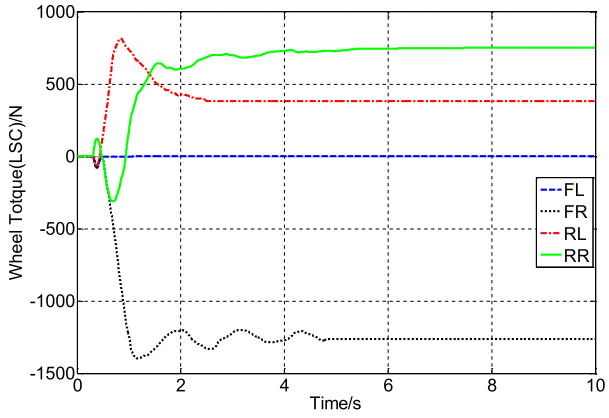

FIGURE 14. Wheel toque(LSC).

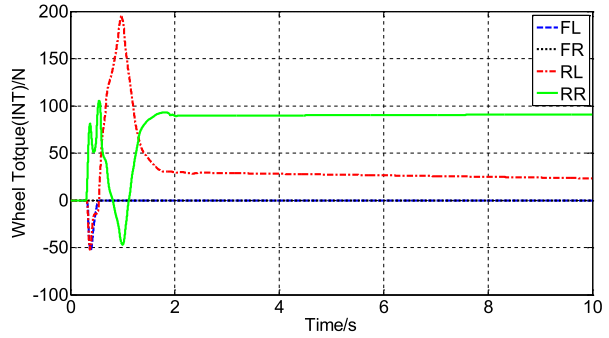

FIGURE 15. Wheel toque(INT).

Figures 13, 14, and 15 show the results of the different control input demands for the vehicle with various different configurations. Compared with the 4WS configuration, the steering demands for the INT case are obviously reduced and the wheel torque demands for LSC are reduced more significantly. But, in the LSC configurations, larger wheel control torques value are required to obtain the same control effect.

VIII. CONCLUSION

In this paper, a flexibility of hierarchical structure scheme is proposed for the vehicle integrated control system. The upper controller is designed to calculate and allocate the aim force using the optimal robust control algorithm. Then, specifically, here focuses on a component of the servo loop to realize self-tuning tyre friction control which adaptive to variation of road condition. On-line identifying system of the Magic Formula parameters is designed to calculate and predict tyre-road friction force using a hybrid GA method and correspondingly acquiring slip ratio for LSC is obtained

using a numerical method. Besides, the vehicle main-servo loop integrated control system is designed consisting of the proposed self-tuning friction controller based the NFTSM. The simulations show that the self-tuning tyre friction controller can effectively tracking the desired target. Compared with individual LSC or 4WS control system, the proposed hierarchical integrated control system can effectively coordinate active steering and active wheel torque, and improve the vehicle handling performances significantly.

ACKNOWLEDGMENT

The first author would like to express appreciation to Dr. Kening Li and Dr. Hai-wei Wang for valuable discussions that improved the quality and presentation of the paper.

REFERENCES

[1] C. K. Huang and M. C. Shih, "Dynamic analysis and control of an anti-lock brake system for a motorcycle with a camber angle," *Vehicle Syst. Dyn.*, vol. 49, no. 4, pp. 639–656, 2011.

[2] J. Yu, Q. Li, and W. Zhou, "Nonlinear robust stabilization of ship roll by convex optimization," *IEEE Access*, to be published, doi: 10.1109/JAS.2016.7510163.

[3] T. Kim, J. Lee, and K. Yi, "Enhanced maximum tire-road friction coefficient estimation based advanced emergency braking algorithm," in *Proc. IEEE Intell. Vehicles Symp. (IV)*, Jul. 2015, pp. 883–888.

[4] S.-T. Peng, C.-C. Cheng, and J.-J. Sheu, "On robust bounded control of the combined wheel slip with integral compensation for an autonomous 4WS4WD vehicle," *Vehicle Syst. Dyn.*, vol. 45, no. 5, pp. 477–503, 2007.

[5] W. Li, T. Potter, and R. P. Jones, "Steering of 4WD vehicles with independent wheel torque control," *Vehicle Syst. Dyn.*, vol. 29, no. S1, pp. 205–218, 1998.

[6] A. Morgando, M. Velardocchia, A. Vigliani, B. G. van Leeuwen, and V. Ondrak, "An alternative approach to automotive ESC based on measured wheel forces," *Vehicle Syst. Dyn.*, vol. 49, no. 12, pp. 1855–1871, 2011.

[7] E. Sabbioni, F. Cheli, and Y. d'alessandro, "Analysis of ABS/ESP control logics using a HIL test bench," SAE Tech. Paper 2011-01-0032, 2011.

[8] H. Xiao, W. Chen, H. Zhou, and J. W. Zu, "Integrated control of active suspension system and electronic stability programme using hierarchical control strategy: Theory and experiment," *Vehicle Syst. Dyn.*, vol. 49, nos. 1–2, pp. 381–397, 2011.

[9] S. Yu, J. Wang, Y. Wang, and H. Chen , "Disturbance observer based control for four wheel steering vehicles with model reference," *IEEE Access*, to be published, doi: 10.1109/JAS.2016.7510220.

[10] M. Nagai, M. Shino, and F. Gao, "Study on integrated control of active front steer angle and direct yaw moment," *JSAE Rev.*, vol. 23, no. 3, pp. 309–315, 2002.

[11] M. Da Lio *et al.*, "Artificial co-drivers as a universal enabling technology for future intelligent vehicles and transportation systems," *IEEE Trans. Intell. Transp. Syst.*, vol. 16, no. 1, pp. 244–263, Feb. 2015.

[12] J. Petit and S. E. Shladover, "Potential cyberattacks on automated vehicles," *IEEE Trans. Intell. Transp. Syst.*, vol. 16, no. 2, pp. 546–556, Apr. 2015.

[13] V. Milanés, S. E. Shladover, J. Spring, C. Nowakowski, H. Kawazoe, and M. Nakamura, "Cooperative adaptive cruise control in real traffic situations," *IEEE Trans. Intell. Transp. Syst.*, vol. 15, no. 1, pp. 296–305, Feb. 2014.

[14] L. Li, D. Wen, N.-N. Zheng, and L.-C. Shen, "Cognitive cars: A new frontier for ADAS research," *IEEE Trans. Intell. Transp. Syst.*, vol. 13, no. 1, pp. 395–407, Mar. 2012.

[15] G. Karagiannis *et al.*, "Vehicular networking: A survey and tutorial on requirements, architectures, challenges, standards and solutions," *IEEE Commun. Surveys Tuts.*, vol. 13, no. 4, pp. 584–616, 4th Quart., 2011.

[16] D. T. Hoang, P. Wang, D. Niyato and E. Hossain, "Charging and discharging of plug-in electric vehicles (PEVs) in vehicle-to-grid (V2G) systems: A cyber insurance-based model," *IEEE Access*, vol. 5, pp. 732–754, 2017.

[17] S. Oncu, J. Ploeg, D. W. N. van, and H. Nijmeijer, "Cooperative adaptive cruise control: Network-aware analysis of string stability," *IEEE Trans. Intell. Transp. Syst.*, vol. 15, no. 4, pp. 1527–1537, Aug. 2014.

[18] M. R. Jabbarpour, H. Zarrabi, J. J. Jung, and P. Kim, "A green ant-based method for path planning of unmanned ground vehicles," *IEEE Access*, vol. 5, pp. 1820–1832, 2017.

[19] R. Hamberg, T. Hendriks, and T. Bijlsma, "Temporal performance of advanced driver assistance systems vis-à-vis human driving behavior in dense traffic," in *Proc. IEEE Int. Conf. Intell. Transp. Syst.*, Sep. 2015, pp. 1292–1297.

[20] M. Edwards, A. Nathanson, J. Carroll, M. Wisch, O. Zander, and N. Lubbe, "Assessment of integrated pedestrian protection systems with autonomous emergency braking (AEB) and passive safety components," *Traffic Injury Prevention*, vol. 16, no. 1, pp. S2–S11, 2015.

[21] S. Geronimi, V. Abadie, and N. Becker, "Methodology to assess and to validate the dependability of an advanced driver assistance system (ADAS) such as automatic emergency braking system (AEBS)," in *Energy Consumption and Autonomous Driving*. Germany: Springer, 2016.

[22] S. Kato, S. Tsugawa, K. Tokuda, T. Matsui, and H. Fujii, "Vehicle control algorithms for cooperative driving with automated vehicles and intervehicle communications," *IEEE Trans. Intell. Transp. Syst.*, vol. 3, no. 3, pp. 155–161, Sep. 2002.

[23] F. You *et al.*, "Trajectory planning and tracking control for autonomous lane change maneuver based on the cooperative vehicle infrastructure system," *Expert Syst. Appl.*, vol. 42, no. 14, pp. 5932–5946, 2015.

[24] S. H. Tamaddoni, S. Taheri, and M. Ahmadian, "Optimal VSC design based on Nash strategy for differential 2-player games," in *Proc. IEEE Int. Conf. Syst., Man Cybern.*, Oct. 2009, pp. 2415–2420.

[25] S. A. Oleksowicz *et al.*, "Regenerative braking strategies, vehicle safety and stability control systems: Critical use-case proposals," *Vehicle Syst. Dyn.*, vol. 51, no. 5, pp. 684–699, 2013.

[26] K. Guo and D. Lu, "UniTire: Unified tire model for vehicle dynamic simulation," *Vehicle Syst. Dyn.*, vol. 45, no. S1, pp. 79–99, 2007.

[27] L. R. Ray, "Nonlinear state and tire force estimation for advanced vehicle control," *IEEE Trans. Control Syst. Technol.*, vol. 3, no. 1, pp. 117–124, Mar. 1995.

[28] H. B. Pacejka, *Tire and Vehicle Dynamics*. London, U.K.: Butterworth, 2012.

[29] S. Sivaraman and M. M. Trivedi, "Looking at vehicles on the road: A survey of vision-based vehicle detection, tracking, and behavior analysis," *IEEE Trans. Intell. Transp. Syst.*, vol. 14, no. 4, pp. 1773–1795, Dec. 2013.

[30] F. Yu, D.-F. Li, and D. A. Crolla, "Integrated vehicle dynamics control—State-of-the art review," in *Proc. IEEE Vehicle Power Propul. Conf.*, Sep. 2008, pp. 1–6.

[31] S. De Pinto, C. Chatzikomis, A. Sorniotti, and G. Mantriota, "Comparison of traction controllers for electric vehicles with on-board drivetrains," *IEEE Access*, to be published, doi: 10.1109/TVT.2017.2664663.

[32] Y. Cho, "The simulation of ABS stopping distance," SAE Tech. Paper 2011-01-0570, 2011.

[33] M. Spiryagin, P. Wolfs, F. Szanto, and C. Cole, "Simplified and advanced modelling of traction control systems of heavy-haul locomotives," *Vehicle Syst. Dyn.*, vol. 53, no. 5, pp. 672–691, 2015.

[34] L. S. Qin, J. J. Hu, H. X. Li, and W. Chen, "Fuzzy logic controllers for specialty vehicles using a combination of phase plane analysis and variable universe approach," *IEEE Access*, vol. 5, pp. 1579–1588, 2017, doi: 10.1109/ACCESS.2017.2656124.

[35] M. Althoff and J. M. Dolan, "Online verification of automated road vehicles using reachability analysis," *IEEE Trans. Robot.*, vol. 30, no. 4, pp. 903–918, Aug. 2014.

[36] Y. Hattori, "Optimum vehicle dynamics control based on tire driving and braking forces (special issue: modeling, analysis and control methods for improving vehicle dynamic behavior)," *R & D Rev. Toyota Crdl*, vol. 38, pp. 23–29, 2002.

[37] O. Mokhiamar and M. Abe, "Simultaneous optimal distribution of lateral and longitudinal tire forces for the model following control," *J. Dyn. Syst., Meas., Control*, vol. 126, no. 4, pp. 753–763, 2004.

[38] L. Li, G. Jia, J. Chen, H. Zhu, D. Cao, and J. Song, "A novel vehicle dynamics stability control algorithm based on the hierarchical strategy with constrain of nonlinear tyre forces," *Vehicle Syst. Dyn.*, vol. 53, no. 8, pp. 1093–1116, 2015.

[39] X. Shen and F. Yu, "Study on vehicle chassis control integration based on a main-loop-inner-loop design approach," *Proc. Inst. Mech. Eng. D, J. Automobile Eng.*, vol. 220, no. 11, pp. 1491–1502, 2006.

[40] D. Li, S. Du, and F. Yu, "Integrated vehicle chassis control based on direct yaw moment, active steering and active stabiliser," *Vehicle Syst. Dyn.*, vol. 46, no. S1, pp. 341–351, 2008.

[41] M. B. Alberding, J. Tjønnås, and T. A. Johansen, "Integration of vehicle yaw stabilisation and rollover prevention through nonlinear hierarchical control allocation," *Vehicle Syst. Dyn.*, vol. 52, no. 12, pp. 1607–1621, 2014.
[42] M. Tanelli, A. Ferrara, and P. Giani, "Combined vehicle velocity and tire-road friction estimation via sliding mode observers," in *Proc. IEEE Int. Conf. Control Appl. (CCA)*, Oct. 2012, pp. 130–135.
[43] R. Tafner, M. Reichhartinger, and M. Horn, "Estimation of tire parameters via second-order sliding mode observers with unknown inputs," in *Proc. 13th Int. Workshop Variable Struct. Syst. (VSS)*, 2014, pp. 1–6.
[44] C. Tricaud and Y. Chen, "An approximate method for numerically solving fractional order optimal control problems of general form," *Comput. Math. Appl.*, vol. 59, no. 5, pp. 1644–1655, 2010.
[45] J.-J. E. Slotine and W. Li, *Applied Nonlinear Control*, vol. 1. Englewood Cliffs, NJ, USA: Prentice-Hall, 1991.
[46] D. Zhao, S. Li, and F. Gao, "A new terminal sliding mode control for robotic manipulators," *Int. J. Control*, vol. 82, no. 10, pp. 1804–1813, 2009.
[47] W. Q. Tang and Y. L. Cai, "High-order sliding mode control design based on adaptive terminal sliding mode," *Int. J. Robust Nonlinear Control*, vol. 23, no. 2, pp. 149–166, 2013.
[48] N. Zhang, *Terminal Sliding Mode Control Theory and Application*. Beijing, China: Science Press, 2011.
[49] P. C. Chen, C. Chen, and W. Chiang, "GA-based modified adaptive fuzzy sliding mode controller for nonlinear systems," *Expert Syst. Appl.*, vol. 36, no. 3, pp. 5872–5879, 2009.
[50] X. Chen, G. Lin, J. Chen, and W. Zhu, "An adaptive hybrid genetic algorithm for VLSI standard cell placement problem," in *Proc. 3rd Int. Conf. Inf. Sci. Control Eng. (ICISCE)*, 2016, pp. 163–167.
[51] L. B. Booker, D. E. Goldberg, and J. H. Holland, "Classifier systems and genetic algorithms," *Artif. Intell.*, vol. 40, nos. 1–3, pp. 235–282, 1989.
[52] F. Jin and W. Chen, "The father of the genetic algorithms–Holland and his scientific work," *J. Dialectics Nature*, vol 29, no. 168, pp. 86–93, 2007.
[53] E. Brookner, P. R. Cornely, Y. F. Lok, "AREPS and TEMPER—Getting familiar with these powerful propagation software tools," in *Proc. Radar Conf. IEEE*, 2007, pp. 1034–1043.
[54] P. Sharma and T. N. Sasamal, "Minimization of combinational digital circuit using genetic algorithm," in *Proc. IEEE Int. Conf. Comput. Intell. Comput. Res. (ICCIC)*, Dec. 2015, pp. 1–4.
[55] H. Han, X.-L. Wu, and J.-F. Qiao, "Nonlinear systems modeling based on self-organizing fuzzy-neural-network with adaptive computation algorithm," *IEEE Trans. Cybern.*, vol. 44, no. 4, pp. 554–564, Apr. 2014.
[56] W. Gong, Z. Cai, J. Yang, X. Li, and L. Jian, "Parameter identification of an SOFC model with an efficient, adaptive differential evolution algorithm," *Int. J. Hydrogen Energy*, vol. 39, no. 10, pp. 5083–5096, 2014.
[57] F. Wang, Z. Chen, P. Stolze, J.-F. Stumper, J. Rodriguez, and R. Kennel, "Encoderless finite-state predictive torque control for induction machine with a compensated MRAS," *IEEE Trans. Ind. Informat.*, vol. 10, no. 2, pp. 1097–1106, May 2014.
[58] T. Ishige, "Adaptive slip control using a brake torque sensor," in *Proc. 9th Int. Symp. Adv. Vehicle Control (AVEC)*, Kobe, Japan, 2008, pp. 36–43.
[59] K. Nam, S. Oh, H. Fujimoto, and Y. Hori, "Estimation of sideslip and roll angles of electric vehicles using lateral tire force sensors through RLS and Kalman filter approaches," *IEEE Trans. Ind. Electron.*, vol. 60, no. 3, pp. 988–1000, Mar. 2013.
[60] H. Asadi, S. Mohamed, D. R. Zadeh, and S. Nahavandi, "Optimisation of nonlinear motion cueing algorithm based on genetic algorithm," *Vehicle Syst. Dyn.*, vol. 53, no. 4, pp. 526–545, 2015.
[61] J. Nocedal and S. J. Wright, *Numerical Optimization*, 2nd ed. Germany: Springer, 2006, pp. 467–540.
[62] L. R. C. Drehmer, W. J. P. Casas, and H. M. Gomes, "Parameters optimisation of a vehicle suspension system using a particle swarm optimisation algorithm," *Vehicle Syst. Dyn.*, vol. 53, no. 4, pp. 449–474, 2015.
[63] K. Li, J. Cao, and F. Yu, "Adaptive longitudinal friction control based on nonsingular and fast terminal sliding mode method," *WSEAS Trans. Syst.*, vol. 11, no. 8, pp. 409–418, 2012.
[64] C. P. Tan, X. H. Yu, and Z. H. Man, "Terminal sliding mode observers for a class of nonlinear systems," *Automatica*, vol. 46, no. 8, pp. 1401–1404, 2010.
[65] V. C. Ilioudis and N. I. Margaris, "PMSM sensorless speed estimation based on sliding mode observers," in *Proc. IEEE Power Electron. Specialists Conf.*, Jun. 2008, pp. 2838–2843.

RONG-HUI ZHANG received the B.Sc. (Eng.) degree from the Department of Automation Science and Electrical Engineering, Hebei University, Baoding, China, in 2003, the M.S. degree in vehicle application engineering from Jilin University, Changchun, China, in 2006, and the Ph.D. (Eng.) degree in mechanical and electrical engineering from the Changchun Institute of Optics, Fine Mechanics and Physics, Chinese Academy of Sciences, Changchun, China, in 2009. He was a Post-Doctoral Researcher with INRIA, Paris, France, in 2011, where he is currently a Research Fellow with the Research Center of Intelligent Transportation Systems, School of Engineering, Sun Yat-sen University, Guangzhou, China. He has authored over ten papers in international journals. His current research interests include computer vision, intelligent control, and ITS.

ZHAO-CHENG HE received the B.E. and Ph.D. degrees from Sun Yat-sen University, Guangzhou, China. He is currently a Professor with the Research Center of Intelligent Transportation Systems, School of Engineering, Sun Yat-sen University. He has authored over ten papers in international journals. His current research interests include intelligent control and ITS.

HAI-WEI WANG received the B.E. and M.S. degrees from Jilin University, Changchun, China, and the Ph.D. degree from the South China University of Technology, Guangzhou, China. She is currently a Research Fellow with the School of Civil Engineering and Transportation, South China University of Technology. She has authored three papers in international journals. Her current research interests include ITS and vehicle control.

FENG YOU received the B.E. degree Guizhou University, Guiyang, China, and the M.S. and Ph.D. degrees from Jilin University, Changchun, China.

He was a Post-Doctoral Researcher with INRIA, Paris, France, in 2011. He was an Associate Professor with the South China University of Technology, Guangzhou, China. He has authored over ten papers in international journals. His interests include advanced driving assistance, computer vision, co-operation control, and visual SLAM.

KE-NING LI received the B.E. degree in communications and transportation from the University of Henan Agricultural University, Henan, China, in 2004, the M.S. degree in vehicle operation engineering from Jilin University, Jilin, in 2007, and the Ph.D. degree in vehicle engineering from the Shanghai Jiao Tong University, Shanghai, in 2014. His research interests are in vehicle system dynamics and control, intelligent vehicle system, and artificial intelligence system.